



PERGAMON

Journal of Geodynamics 30 (2000) 401–421

JOURNAL OF
GEODYNAMICS

www.elsevier.nl/locate/jgeodyn

Seismotectonics and rates of active crustal deformation in the Burmese arc and adjacent regions

M. Radha Krishna*, T.D. Sanu

Department of Marine Geology and Geophysics, School of Marine Sciences, Cochin University of Science and Technology, Fine Arts Avenue, Cochin 682 016, India

Received 15 December 1998; accepted 15 September 1999

Abstract

The close vicinity of the Burmese subduction zone to the Himalayan collision zone across northeast India produces complex tectonics giving rise to a high level of seismicity. Using the hypocentral data of shallow earthquakes ($h \leq 70$ km) for the period 1897–1995, a large number of focal mechanism solutions and other geophysical data in correlation with major morphotectonic features in the Burmese arc and the adjoining areas, we identified 12 broad seismogenic zones of relatively homogeneous deformation. Crustal deformation rates have been determined for each one of these sources based on summation of moment tensors. The results indicate that along the Kopili–Bomdila fault zone in eastern Himalaya, the deformation is taken up as a compression of 0.12 ± 0.01 mm/yr along $N16^\circ$ and an extension of 0.05 ± 0.004 mm/yr along $N104^\circ$ direction. The deformation velocities show a NS compression of 18.9 ± 2.5 mm/yr and an EW extension of 17.1 ± 2.2 mm/yr in the Shillong Plateau region, while a compression of 5.4 ± 2.8 mm/yr along $N33^\circ$ is observed in the Tripura fold belt and the Bengal basin region. The vertical component in the Shillong Plateau shows crustal thickening of 2.4 ± 0.3 mm/yr. The deformation velocities in Indo–Burman ranges show a compression of 0.19 ± 0.02 mm/yr along $N11^\circ$ and an extension of 0.17 ± 0.01 mm/yr along $N101^\circ$ in the Naga hills region, a compression of 3.3 ± 0.4 mm/yr along $N20^\circ$ and an extension of 3.1 ± 0.36 mm/yr along $N110^\circ$ in the Chin hills region and a compression of 0.21 ± 0.3 mm/yr in $N20^\circ$ and an extension of 0.18 ± 0.03 mm/yr along $N110^\circ$ in the Arakan–Yoma region. The dominance of strike-slip motions with the P axis oriented on an average along $N17^\circ$ indicate that the Burma platelet may be getting dragged along with the Indian plate and the motion of these two together is accommodated along the Sagaing fault. The velocities estimated along Sagaing transform fault in the back-arc region suggest that the deformation is taken up as an extension of 29.5 ± 4.7 mm/yr along $N344^\circ$ and a compression of 12.4 ± 1.9 mm/yr along $N74^\circ$ in the northern part of the fault zone, and a compression of 17.4 ± 2.3 mm/yr along $N71^\circ$ and an extension of 59.8 ± 8.0 mm/

* Corresponding author.

yr along N341° in the southern part of the fault zone. The average shear motion of about 13.7 mm/yr is observed along the Sagaing fault. The deformation observed in the southern part of the syntaxis zone along the Mishmi thrust indicate a compression of 0.63 ± 0.08 mm/yr in N58° and an extension of 0.6 ± 0.07 mm/yr in N328° direction. The region of Shan Plateau, west of Red River fault, shows a compression of 17.7 ± 2.6 mm/yr along N36° and an extension of 16.1 ± 2.4 mm/yr along N126°. © 2000 Published by Elsevier Science Ltd. All rights reserved.

1. Introduction

The Burmese arc lying in the immediate vicinity of the Himalayan collision zone and also as a constituent of the plate convergence zone extending southward along the Andaman and Indonesian arcs, forms an important transition between them. Mitchell and McKerrow (1975) ascribed the evolution of the arc to a process of eastward subduction of the Indian plate at the Asian continental margin from at least Late Cretaceous. The Benioff zone is characterized by shallow and intermediate focus earthquakes (Mukhopadhyay and Dasgupta, 1988; Ni et al., 1989). Satyabala (1998) inferred active subduction of the Indian plate beneath the Burmese arc. Curray et al. (1979) proposed that a lenticular plate, the Burma plate, forms a structural province in the area between the Arakan–Yoma to the west and the high lands to the east. The region north of 22°N is tectonically more complicated characterized by widespread occurrence of earthquakes both along the arc and in the surrounding regions such as parts of northeast India, eastern Himalaya and Shan Plateau. The seismotectonics of northeast India is attributed to south directed overthrusting from the north due to collision tectonics at the Himalayan arc, and northwest directed overthrusting due to subduction tectonics at the Burmese arc (Verma et al., 1976a; Mukhopadhyay and Dasgupta, 1988). Various morphotectonic features of the Burmese arc and adjacent regions are shown in Fig. 1.

In the present study, we utilise the hypocentral data of shallow earthquakes (depth $h \leq 70$ km) of more than 100 years and a large number of focal mechanism solutions, to identify broad seismogenic sources within the Burmese arc and adjacent regions and to study the active crustal deformation. The method is based on summation of the moment tensor elements of shallow earthquakes.

2. Method and data analysis

The method of analysis followed here is one proposed by Papazachos and Kiratzi (1992) which is based on the formulations of Kostrov (1974), Molnar (1979) and Jackson and McKenzie (1988). The method was subsequently applied in seismically active regions by Papazachos et al. (1992), Kiratzi (1993), Kiratzi and Papazachos (1995) and Papazachos and Kiratzi (1996). We briefly mention the method below.

The average strain rate tensor $\dot{\epsilon}_{ij}$, which is the symmetric part of the velocity gradient tensor, is calculated by the following relation (Kostrov, 1974):

$$\dot{\epsilon}_{ij} = \frac{1}{2\mu V} \frac{\sum_{n=1}^N M_{ij}}{T} = \frac{1}{2\mu V} \dot{M}_0 \bar{F}_{ij} \quad i, j = 1, 2, 3 \quad (1)$$

Where V is the deformed volume, $\sum M_{ij}$ is the sum of the moment tensors of the earthquakes that occurred within the volume in T years, μ is the rigidity of crustal rocks, \dot{M}_0 is the seismic moment rate, and \bar{F}_{ij} is a focal mechanism tensor calculated by averaging over N mechanisms, where F_{ij}^n is a function of strike, dip and rake of the focal mechanism (Aki and Richards, 1980).

The rate of moment release \dot{M}_0 , used in the above equation is calculated from Molnar (1979) as:

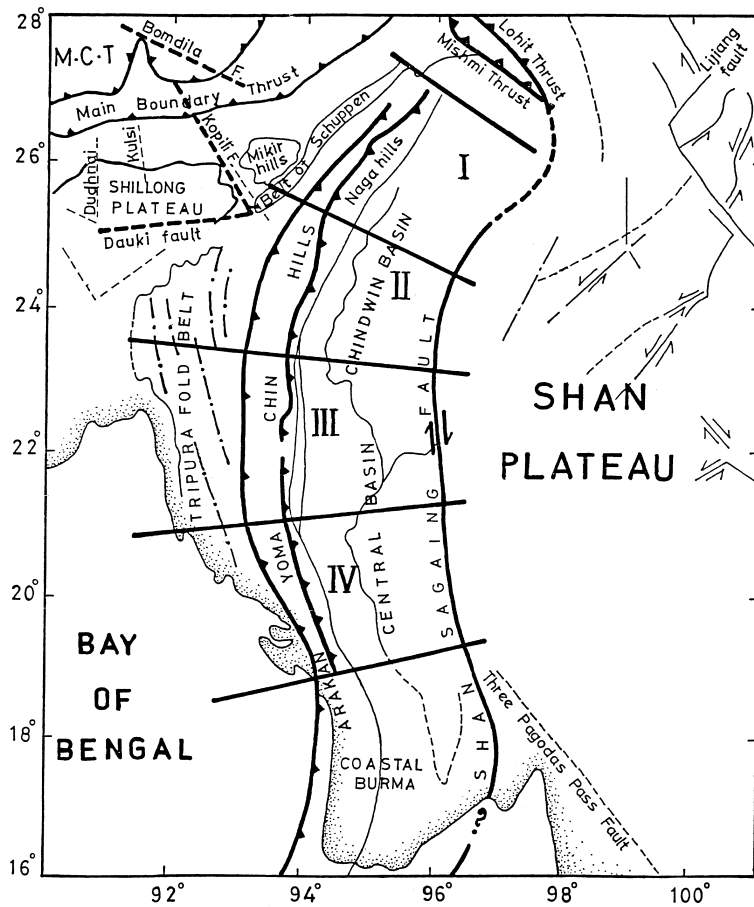


Fig. 1. Tectonic map of the Burmese arc and adjacent regions modified and redrawn from Nandy (1981). The zones marked I–IV are the broad segmentation of the Burmese arc based on seismicity patterns and morphotectonic trends by Mukhopadhyay and Dasgupta (1988). Tectonic details in the Shan Plateau region are adopted from Haines and Holt (1993). MCT — Main Central Thrust.

$$\dot{M}_0 = \frac{A}{1-B} M_{0, \max}^{(1-B)} \quad (2)$$

where $M_{0, \max}$ is the scalar moment of the largest observed earthquake in the region and

$$A = 10 \left[a + \left(\frac{bd}{c} \right) \right] \quad \text{and} \quad B = \frac{b}{c}$$

where a and b are the constants of the Gutenberg–Richter relation and c and d are the constants of moment–magnitude relation applicable to the area. Finally, the integrated rates of motion U_{ij} normal and parallel to the zone boundary as well as vertically are calculated by the following relations.

$$U_{ij} = \frac{1}{2\mu l_k l_j} \dot{M}_0 \bar{F}_{ij} \quad i = 1, 2, 3 \quad i \neq j, j \neq k, k \neq i \quad (3)$$

$$U_{12} = \frac{1}{2\mu l_1 l_3} \dot{M}_0 \bar{F}_{12} \quad (4)$$

$$U_{i3} = \frac{1}{2\mu l_1 l_2} \dot{M}_0 \bar{F}_{i3} \quad i = 1, 2 \quad (5)$$

where l_1 , l_2 are length and width of the deforming zone and l_3 is the depth extend of the seismogenic layer. The reference system in Eqs. (1), (3)–(5) is the zones local system (length/width/depth). Since \bar{F}_{ij} is usually calculated in the north/east/down system, a rotation in the zone's system is necessary.

3. Seismogenic zones and moment release rates

3.1. Identification of seismogenic sources

Many previous workers have studied seismicity in relation to overall tectonics of the region and their studies gave valuable information on seismotectonics, subduction process and plate kinematic setting of the Burmese arc and adjacent regions (Santo, 1969; Fitch, 1970, 1972; Chandra, 1975, 1978; Verma et al., 1976a; LeDain et al., 1984; Kayal, 1987, 1996; Mukhopadhyay and Dasgupta, 1988; Chen and Molnar, 1990; Nandy and Dasgupta, 1991; Holt et al., 1991; Ravikumar and Rao, 1995; Satyabala, 1998). Detailed investigations on regional geology, morphotectonics and their relation to gravity anomalies in this region have been made by Verma et al. (1976b), Nandy (1986) and Mukhopadhyay and Dasgupta (1988). Based on the morphotectonic trends and the seismicity pattern, Mukhopadhyay and Dasgupta (1988) divided the Burmese arc region into four sectors, Sector I corresponding to the Naga hills area in the north to Sector IV covering Arakan–Yoma region of Coastal Burma in the south (Fig. 1). Based on detailed seismotectonic evaluation of northeast India, Kayal (1996) identified five broad tectonic zones such as the Himalayan collision zone, Indo-Burma

subduction zone, the Syntaxis zone (Mishmi hills), Shillong Plateau and Assam valley area, and the Bengal basin–Tripura fold belt area. Studies by Nandy and Dasgupta (1991) and Kayal et al. (1993) reveal that the Kopili–Bomdila fault zone is seismically the most active region in the eastern Himalayas with many of the events displaying strike-slip motion along the NW nodal plane oblique to the Himalayan trend. East of the Indo-Burman ranges, the Sagaing fault in the back arc region is seismically very active. LeDain et al. (1984) and Ni et al. (1989) suggested that most of the right-lateral slip of India is accommodated along the Sagaing fault. Further east, the Shan Plateau belonging to the Asian plate is also seismically active and intraplate deformation in this region is distributed over several left-lateral faults (Haines and Holt, 1993) (Fig. 1).

Since the region under investigation is very large, it has to be divided into seismogenic sources of relatively homogeneous deformation. For this purpose, we compiled the hypocentral data of all shallow earthquakes ($h \leq 70$ km) for the Burmese arc and adjacent regions from ISC and PDE listings. Events before 1964 were considered from Gutenberg and Richter (1954) and Rothe (1969). The data set also include the events compiled by Gupta et al. (1986) for northeast India and large earthquakes in the eastern Himalayas and northeast India by Satyabala and Gupta (1996). We considered all events of $M_s \geq 4.5$ for the present analysis. For few events the M_s value is obtained from m_b by using m_b – M_s relation derived for this region. The magnitudes estimated by Gutenberg and Richter (1954) and Rothe (1969) are equivalent to 20-s M_s (Geller and Kanamori, 1977). The seismicity map prepared for the Burmese arc and the adjacent regions is shown in Fig. 2.

Further, we compiled 92 focal mechanism solutions of events occurring in this region from various sources. The mechanisms are mostly obtained from quarterly reports of Harvard CMT solutions published by Dziewonski and other co-workers in the Physics of the Earth and Planetary Interior. A good number of reliable solutions are also obtained from Chen and Molnar (1990) for the Shillong Plateau and Indo-Burman ranges, from Nandy and Dasgupta (1991) for Northeast India and from Mukhopadhyay and Dasgupta (1988) for the Burma region. Six composite fault plane solutions given by Kayal (1987) and Mukhopadhyay et al. (1993) for the Shillong Plateau are also considered for the present study. The source parameters of all the 92 mechanisms are listed in Table 1 and they are plotted as shown in Fig. 3. By considering the previous seismotectonic studies, a careful analysis of the seismicity map and focal mechanism solutions in correlation with various tectonic features of the region has been attempted. The analysis indicate that the Burmese arc and surrounding regions could be divided into 12 broad seismogenic sources. The boundaries for each source are defined based on the epicentral area and the morphotectonic trends. The Indo-Burman ranges in which most of the mechanisms show either thrust or strike-slip faulting is considered as a single seismic belt but because of its convex geometry, depending on the strike direction (Mukhopadhyay and Dasgupta, 1988) the Indo-Burman ranges has been divided into three sources (4, 5 and 6). Similarly, Sagaing transform has also been considered as a single seismic belt divided into two sources (10 and 11) because of its difference in orientation from north to south. For each of these two seismic belts, the mechanisms of all sources falling in that belt are utilised for estimating a single focal mechanism tensor \bar{F} for that belt. The length l_1 , width l_2 , azimuth and the identified tectonic zone for each of these 12 seismogenic sources are listed in Table 2.

3.2. Moment release rates

The rates of seismic moment release for each seismogenic source can be estimated by using Eq. (2) presented in Section 2. The advantage of this formula is that the full record of seismicity both historical and of the present century can be used in any given region. The most important parameters in this calculation are a and b values of the Gutenberg–Richter relation. For reliable estimation of these parameters we have adopted the “mean value method” used by Papazachos (1990) which was originally proposed by Milne and Davenport (1969) for earthquake risk analysis. According to this method, in a given source region, the time interval of available data is divided into subintervals and for each subinterval a minimum magnitude M_{\min} is defined above which the data of the subinterval are complete. For example, t and M_{\min} for source 2 in Table 2 implies that data are complete for earthquakes with $M_s \geq 7.1$ from 1897–1995, for $M_s \geq 5.6$ from 1932–1995 and for $M_s \geq 4.5$ from 1964–1995. The number of events for each magnitude during the whole time period can be obtained from the number of

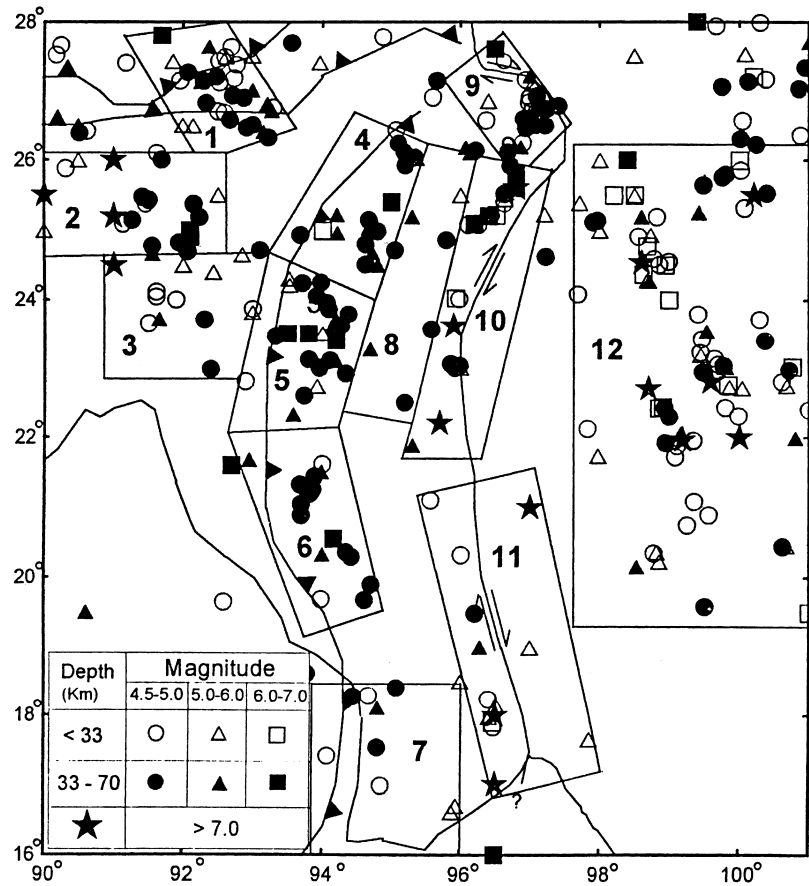


Fig. 2. Seismicity map of the Burmese arc and adjacent regions. Those events with $h \leq 70$ km have been considered for the present study. The region is divided into 12 broad seismogenic sources. Details are discussed in text.

Table 1

Source parameters of 92 focal mechanism solutions shown in Fig. 3. The location, depth and magnitude for each event is considered from ISC and PDE listings. The faulting type is classified based on the calculation of “mean slip angle” suggested by Ravikumar et al. (1996). N — normal, S — Strike slip, T — Thrust. Mechanisms indicated with a star are composite fault plane solutions based on micro earthquake investigations in Shillong Plateau (Kayal, 1987; Mukhopadhyay et al., 1993)

S. No.	Source	Date		Latitude °N	Longitude °E	Depth (km)	Magnitude M_s	Seismic Moment ($\times 10^{24}$)	Strike	Dip	Slip	Type of faulting	Reference ^a
1	2	1963	6 19	25.00	92.10	51	—	—	57	80	42	S	8
2	2	1963	6 21	24.90	92.10	53	—	—	238	88	-70	S	8
3	5	1964	1 22	22.33	93.58	60	—	—	14	74	-66	N	2
4	1	1964	9 1	27.12	92.26	33	—	—	22	64	-14	S	3
5	4	1965	2 18	25.00	94.30	36	5.4	—	220	60	216	S	8
6	1	1965	12 9	27.40	92.50	29	5.1	—	102	62	92	T	5
7	1	1966	9 26	27.49	92.61	20	—	—	314	56	41	S	3
8	8	1967	1 30	26.10	96.14	39	—	—	36	78	173	S	2
9	6	1967	2 15	20.33	93.99	51	—	—	38	54	6	S	2
10	1	1967	9 15	27.42	91.86	19	—	—	68	64	-153	S	3
11	2	1968	6 12	24.83	91.94	39	5.3	—	132	60	135	S	8
12	3	1968	12 27	24.12	91.61	0	—	—	140	72	138	S	8
13	3	1969	1 25	22.98	92.40	49	—	—	348	18	63	T	2
14	4	1969	4 28	25.93	95.20	60	—	—	24	70	-66	N	2
15	1	1969	6 30	26.93	92.71	44	—	—	68	50	60	T	5
16	9	1970	3 10	26.83	96.98	24	—	—	336	86	-170	S	3
17	5	1970	5 29	23.96	94.06	49	5.1	—	151	70	158	S	8
18	4	1970	7 29	26.02	95.37	68	—	—	11	76	-136	S	2
19	3	1971	2 2	23.71	91.66	37	—	—	119	36	90	T	8
20	10	1971	5 30	25.20	96.40	40	6.1	—	37	80	169	S	2
21	10	1971	5 31	25.22	96.51	22	6.1	—	17	70	-174	S	2
22	1	1971	7 17	26.41	93.15	52	5.1	2.60	79	60	46	T	8
23	10	1971	10 10	23.00	95.92	46	—	—	324	78	-32	S	2
24	10	1971	10 14	23.06	95.86	47	—	—	329	84	-32	S	2
25	4	1971	12 29	25.17	94.72	46	—	—	176	70	180	S	8
26	5	1973	5 31	24.31	93.52	1	5.7	21.00	253	80	13	S	8
27	8	1973	7 27	23.27	94.49	60	—	—	10	12	122	T	2
28	6	1974	4 5	21.33	93.68	47	—	—	316	84	36	S	2
29	5	1975	5 21	23.86	94.09	51	—	—	243	40	0	S	8
30	9	1975	7 23	26.58	96.36	22	4.7	—	88	66	-15	S	2

(continued on next page)

Table 1 (continued)

S. No.	Source	Date			Latitude °N	Longitude °E	Depth (km)	Magnitude M_s	Seismic Moment ($\times 10^{24}$)	Strike	Dip	Slip	Type of faulting	Reference ^a
31	5	1975	12	13	23.62	94.27	62	–	–	5	9	136	T	2
32	12	1976	5	31	24.37	98.62	25	6.2	–	39	70	–130	S	6
33	12	1976	6	9	24.94	98.74	13	5.9	–	41	30	–89	N	6
34	12	1976	7	21	24.78	98.68	4	6.3	–	39	36	–90	N	6
35	9	1976	8	12	26.70	97.04	31	–	6.10	316	42	–168	S	3
36	6	1977	5	12	21.68	92.96	39	5.7	10.00	216	72	3	S	1
37	5	1977	10	13	23.47	93.33	61	–	1.60	145	41	–171	S	1
38	1	1978	4	19	27.67	92.68	51	4.4	–	56	80	–5	S	3
39	7	1978	9	30	16.60	95.88	7	5.7	5.10	17	76	–168	S	1
40	9	1979	4	25	27.43	96.63	24	–	–	316	70	–34	S	3
41	7	1979	10	3	18.11	94.80	41	–	3.20	334	76	–97	N	1
42	10	1979	11	25	25.21	96.32	32	5.1	0.90	357	79	–175	S	1
43	9	1979	12	21	27.10	97.04	32	5.1	1.10	323	51	106	T	1
44	5	1980	11	20	22.74	93.92	30	5.1	0.78	345	76	78	T	1
45	8	1981	6	30	22.50	95.19	42	–	0.28	7	40	145	T	1
46	12	1981	8	14	25.15	97.96	38	4.6	0.90	33	63	–52	N	1
47	10	1981	8	16	25.52	96.63	38	4.7	0.49	298	66	–7	S	1
48	13	1981	9	12	21.09	99.36	19	4.8	0.63	77	60	13	S	1
49	1	1983	2	2	26.90	92.88	42	–	–	315	72	158	S	3
50	4	1983	8	30	25.04	94.67	68	–	4.04	255	74	31	S	1
51	1	1984	3	21	26.76	93.29	15	–	–	326	66	14	S	3
52	13	1984	4	23	22.06	99.18	8	5.6	9.01	84	69	14	S	1
53	5	1984	5	6	24.22	93.53	32	5.8	12.00	252	76	18	S	8
54	1	1984	9	22	26.49	92.15	29	5	–	301	86	33	S	3
55	9	1984	11	28	26.65	97.08	4	5.7	3.66	210	74	144	S	1
56	3	1984	12	30	24.66	92.85	4	–	13.00	350	45	122	T	1
57	8	1985	4	24	26.18	96.08	46	5.1	0.88	182	58	113	T	1
58	12	1985	9	5	25.40	97.71	28	5.1	2.15	14	65	177	S	1
59	3	1986	2	8	23.87	93.00	30	4.9	1.50	224	62	15	S	1
60	2	1986	2	19	25.10	91.13	7	4.9	1.10	340	50	180	S	1
61	5	1986	7	26	23.72	94.19	38	5.1	1.70	36	76	162	S	1
62	9	1986	11	1	26.85	96.40	11	5	0.70	28	45	132	T	1
63	2	1988	2	6	24.67	91.56	33	5.8	6.70	147	82	166	S	1
64	7	1988	2	19	18.41	95.07	57	–	0.74	329	78	–82	N	1

65	6	1988	10	23	20.30	94.41	66	-	0.53	313	68	-105	N	1
66	13	1988	11	6	22.80	99.59	18	7.3	370.00	64	84	12	S	1
67	13	1988	11	7	23.43	99.49	18	-	0.87	122	55	40	S	1
68	13	1988	11	15	23.15	99.65	18	4.8	1.00	63	90	20	S	1
69	13	1988	11	30	22.76	99.84	15	6	15.00	76	87	-15	S	1
70	9	1989	2	12	26.20	96.90	20	4.9	0.95	295	60	24	S	1
71	3	1989	4	13	24.40	92.43	18	5	1.70	291	6	20	T	1
72	13	1989	5	7	23.54	99.54	33	5.6	3.30	68	79	15	S	1
73	13	1989	9	28	20.36	98.82	11	5.7	6.20	76	72	-1	S	1
74	13	1989	9	30	20.23	98.86	13	5.6	5.30	85	78	-168	S	1
75	6	1989	12	2	21.21	93.82	49	4.6	1.10	196	42	-50	N	1
76	6	1989	12	8	21.19	93.80	59	4.5	1.70	213	38	-31	S	1
77	10	1991	1	5	23.61	95.90	20	7.1	310.00	2	68	166	S	1
78	13	1992	4	23	22.44	98.90	12	6.1	16.00	262	79	-13	S	1
79	13	1992	4	23	22.42	98.85	10	6.3	19.00	252	84	--22	S	1
80	10	1992	6	15	24.03	95.93	17	6.3	31.00	8	69	-173	S	1
81	10	1994	1	11	25.23	97.20	10	5.9	9.10	73	52	-113	N	4
82	6	1994	5	29	20.56	94.16	36	6.2	42.00	224	31	-6	S	4
83	6	1994	8	3	21.51	93.98	34	5.1	5.20	211	88	3	S	4
84	11	1994	8	19	17.97	96.42	12	5.6	4.80	194	66	176	S	4
85	10	1994	11	21	25.54	96.66	14	5.9	5.70	33	71	165	S	4
86	1	1995	2	17	27.64	92.37	39	5.1	1.80	322	46	-172	S	1
*87	2	1982	-	-	25.65	91.75	-	-	-	26	60	99	T	7
*88	2	1984	-	-	25.75	90.85	-	-	-	15	45	43	T	7
*89	2	1984	-	-	25.50	91.00	-	-	-	92	60	90	T	9
*90	2	1984	-	-	25.55	90.75	-	-	-	36	72	52	S	9
*91	2	1984	-	-	25.85	90.75	-	-	-	42	56	14	S	9
*92	2	1984	-	-	25.70	91.15	-	-	-	38	48	13	S	9

^a 1 — Harvard CMT Solutions; 2 — Mukhopadhyay and Dasgupta (1988); 3 — Nandy and Dasgupta (1991); 4 — Sipkin and Zirbes (1996); 5 — Verma and Krishnakumar (1987); 6 — Biswas and Dasgupta (1986); 7 — Kayal (1987); 8 — Chen and Molnar (1990); 9 — Mukhopadhyay et al. (1993).

earthquakes in the corresponding magnitude ranges for each subinterval and multiplied by the ratio of total time interval to subinterval. Having the number of events for each magnitude and for the whole time period, the cumulative frequency and hence a and b values can be easily estimated. The standard errors in a and b values are also calculated which will be used for estimating uncertainties in moment rates. The a and b values and total number of earthquakes for each source region are tabulated in Table 2. As can be seen from the table, the b -values range between 0.4 and 1.1 with values less than 0.5 in four sources. Molnar (1979) pointed out that such low values sometimes could be observed in very small areas or shorter time periods. However, except for source 3, the other sources (2, 10 and 11), show very low errors in the

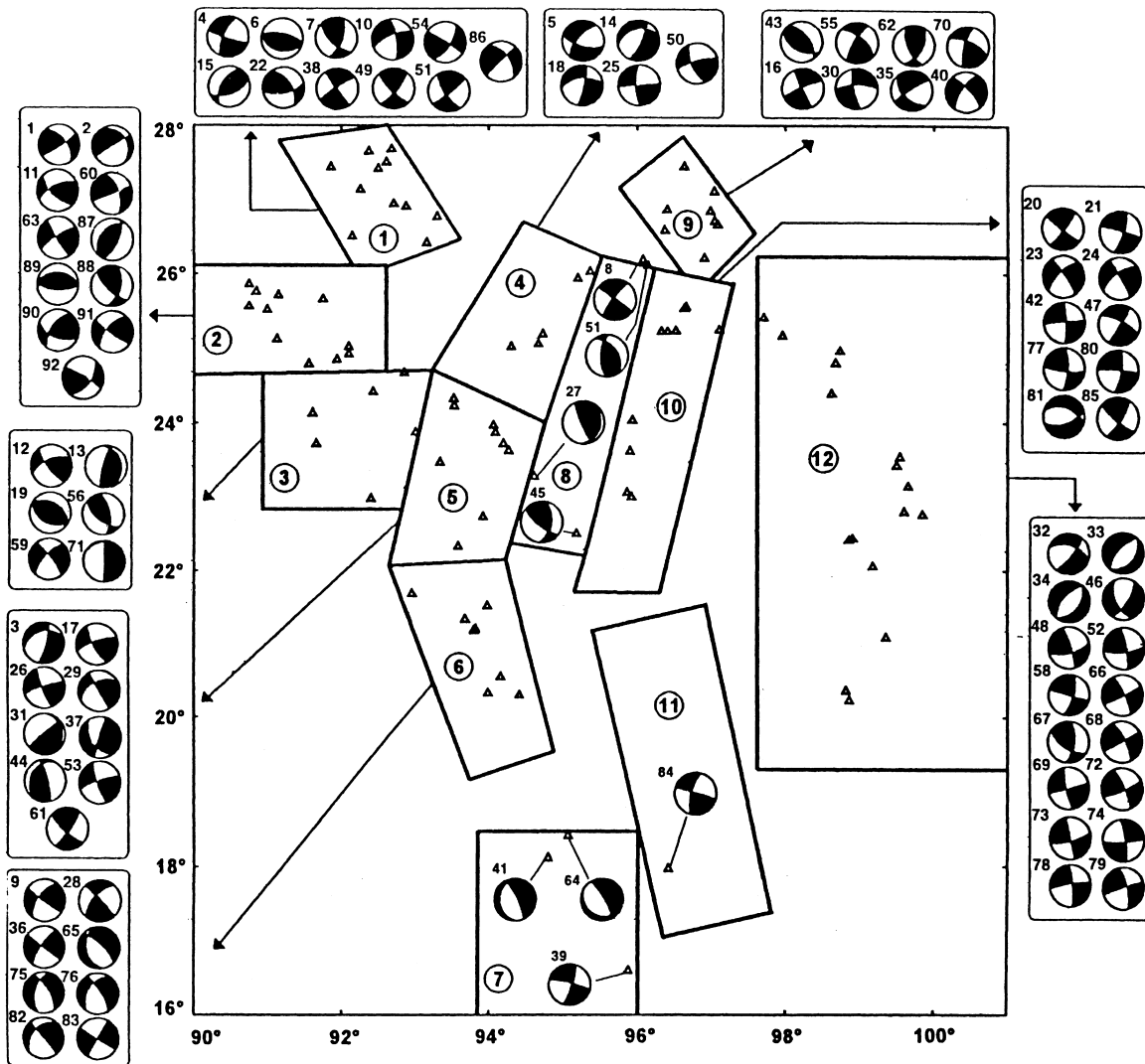


Fig. 3. Map showing the focal mechanism solutions pertaining to each of the 12 seismogenic sources identified in the present study. The number for each solution refers to Table 1.

Table 2

Parameters used in the calculation of deformation of each seismogenic source identified in the present study. l_1 and l_2 are length and width of the source. Az — Azimuth of each deforming area. $M_{s, \max}$ — Maximum magnitude ever observed in each source for the complete data. a and b — Annual a and b values of the Gutenberg–Richter relation, respectively, based on the method of Milne and Davenport (1969) with errors in their estimate. t and M_{\min} refer to data completeness for each source as discussed in the text

Source No.	Region name	l_1 (km)	l_2 (km)	t	M_{\min}	Azimuth ($^{\circ}$ N)	a	b	Total no. of events	$M_{s, \max}$	No. of events ($M_s \geq 6.0$)	$\dot{M}_0 \times 10^{24}$ (dyne cm/yr)
1	Kopili–Bomdila fault zone	165.0	87.0	1932	5.5	160	4.87 ± 0.17	1.08 ± 0.07	28	6.30	1	1.52
2	Shillong Plateau	307.1	144.4	1964	4.5	90	1.61 ± 0.06	0.45 ± 0.02	19	8.00	5	214.19
				1897	7.1							
3	Tripura fold belt and Bengal basin	233.2	198.0	1932	5.6	90	1.43 ± 0.36	0.46 ± 0.14	15	7.60	1	37.92
				1964	4.5							
				1918	7.6							
4	Indo-Burman ranges (Naga hills)	251.4	153.5	1932	5.6	25	3.53 ± 0.11	0.83 ± 0.05	17	6.25	2	1.50
				1964	4.7							
				1930	5.5							
5	Indo-Burman ranges (Chin hills)	240.9	159.1	1965	4.6	9	2.24 ± 0.04	0.55 ± 0.01	19	7.20	5	27.01
				1938	5.6							
6	Indo-Burman ranges (Arakan–Yoma)	319.5	139.6	1964	4.7	169	2.85 ± 0.18	0.70 ± 0.08	15	6.20	1	1.55
				1977	4.5							
7	Coastal Burma	256.8	256.6	1978	4.6	0	3.80 ± 0.17	0.93 ± 0.07	9	5.70	0	0.39
8	Chindwin fore-arc basin	445.2	100.5	1931	5.5	16	3.88 ± 0.30	0.98 ± 0.13	9	5.60	0	0.26
				1931	5.5							
				1964	4.6							
9	Mishimi Thrust zone	193.8	117.2	1955	5.5	145	2.81 ± 0.14	0.66 ± 0.06	25	6.40	4	4.01
				1964	4.6							
10	Shan–Sagaing transform (North)	481.9	128.4	1931	5.5	10	1.85 ± 0.05	0.46 ± 0.02	24	7.60	9	104.03
				1964	4.5							
11	Shan–Sagaing transform (South)	501.6	156.3	1912	7.3	170	1.31 ± 0.07	0.40 ± 0.02	15	7.90	3	199.80
				1931	5.6							
				1964	4.5							
12	Shan Pleateau	722.0	302.5	1923	7.1	0	2.83 ± 0.04	0.57 ± 0.01	76	7.30	18	98.28
				1931	5.6							
				1963	4.5							

estimated b value. Another important parameter in the calculation of moment release rate is $M_{0, \max}$, the seismic moment related to the maximum magnitude event in a given source. Molnar (1979) pointed out that the frequency of occurrence of earthquakes can be expressed in terms of the rate of slip on a fault and of the largest seismic moment likely to occur in that region. The recurrence relation for the seismic moment when coupled with the knowledge of faulting for major earthquakes in any region can constrain the estimation of $M_{0, \max}$ with little uncertainty. Alternatively, Papazachos and Kiratzi (1992) proposed that $M_{0, \max}$ can be directly estimated from $M_{s, \max}$ using the appropriate M_s – M_0 relation, where, $M_{s, \max}$ is the maximum magnitude ever observed from the complete record of seismicity in that region. As mentioned by them, the errors in M_s value for historical earthquakes could be 0.35. For calculation of c and d values in the magnitude–moment relation, the seismic moments of earthquakes with $M_s \geq 5.5$ and depth ≤ 50 km listed in Table 1 are utilised. Since the slope c of the magnitude–moment relation is very sensitive to errors in M_s value, by considering c equal to 1.5 as defined by Kanamori and Anderson (1975), we calculated the value d (intercept) from the observed data. The magnitude–moment relation shown in Fig. 4 gives a value of $d = 16.16$ with an *rms* error of 0.26 with the observed data. Since this relation satisfactorily explains the observed data, we used it for converting the $M_{s, \max}$ to $M_{0, \max}$. The $M_{s, \max}$ and moment release rate \dot{M}_0 calculated for each source are shown in Table 2.

4. Strain rates and deformation velocities

Following the analysis presented in Section 2, the strain rates and velocities for each source are calculated using (1) and (3)–(5). Papazachos and Kiratzi (1992) carried out a detailed error analysis of strain rates and velocity tensors using the Monte-Carlo simulation technique. They observed that the errors in \dot{M}_0 influence only the magnitude of strain and velocity rates, while errors in \bar{F} contribute only in the direction of eigen values of velocity and strain rate tensor. In order to estimate uncertainties in the magnitude of observed velocities for each source, we estimated errors in \dot{M}_0 using Monte-Carlo simulation method. The method adopted is briefly mentioned here.

It can be seen from Eq. (2) that errors in \dot{M}_0 are contributed from errors in a , b , c , d and $M_{s, \max}$. Assuming random errors in these parameters with known medians and standard deviations, Gaussian deviates can be introduced. If \mathbf{m} is the vector of mean values of the parameters, the new parameter vector $\mathbf{P} = (a, b, c, d, M_{s, \max})$ can be repeatedly obtained by using

$$\mathbf{P} = \mathbf{Cz} + \mathbf{m} \quad (6)$$

where, \mathbf{z} is the standard Gaussian random vector with deviates produced using the polar Box–Mueller transform, \mathbf{C} is the unique lower triangular matrix such that $\mathbf{V} = \mathbf{C} \times \mathbf{C}^T$ when \mathbf{V} is the covariance matrix of the parameter vector. The standard errors in a and b estimated from data for each source are given in Table 2. A value of 0.35 is assigned to the standard error in $M_{s, \max}$. The standard error in c value is assumed as 0.05 (Papazachos and Kiratzi, 1992) and the *rms* error in the fit of magnitude–moment relation of 0.26 is assigned to standard error in d . Using Eq. (6), the new parameters can be obtained in each repetition in order to estimate

the new value of \dot{M}_0 and corresponding velocity tensor. These set of values can be used to obtain the mean and standard deviation. Table 3 shows the components of strain rate tensor $\dot{\epsilon}$ and velocity tensor U and the eigen system of velocity tensor with errors in eigen values for the 12 seismogenic sources in the region. The thickness of the seismogenic layer l_3 is considered for different sources based on previous studies on crustal structure and depth of seismic activity. The thickness $l_3 = 50$ km for source 1 (Kayal et al., 1993), $l_3 = 40$ km for source 2 (Kayal, 1987), $l_3 = 35$ km for source 3 and $l_3 = 25$ km for sources 4 to 11 (Mukhopadhyay and Dasgupta, 1988) and $l_3 = 15$ km for source 12 (Holt and Haines, 1993).

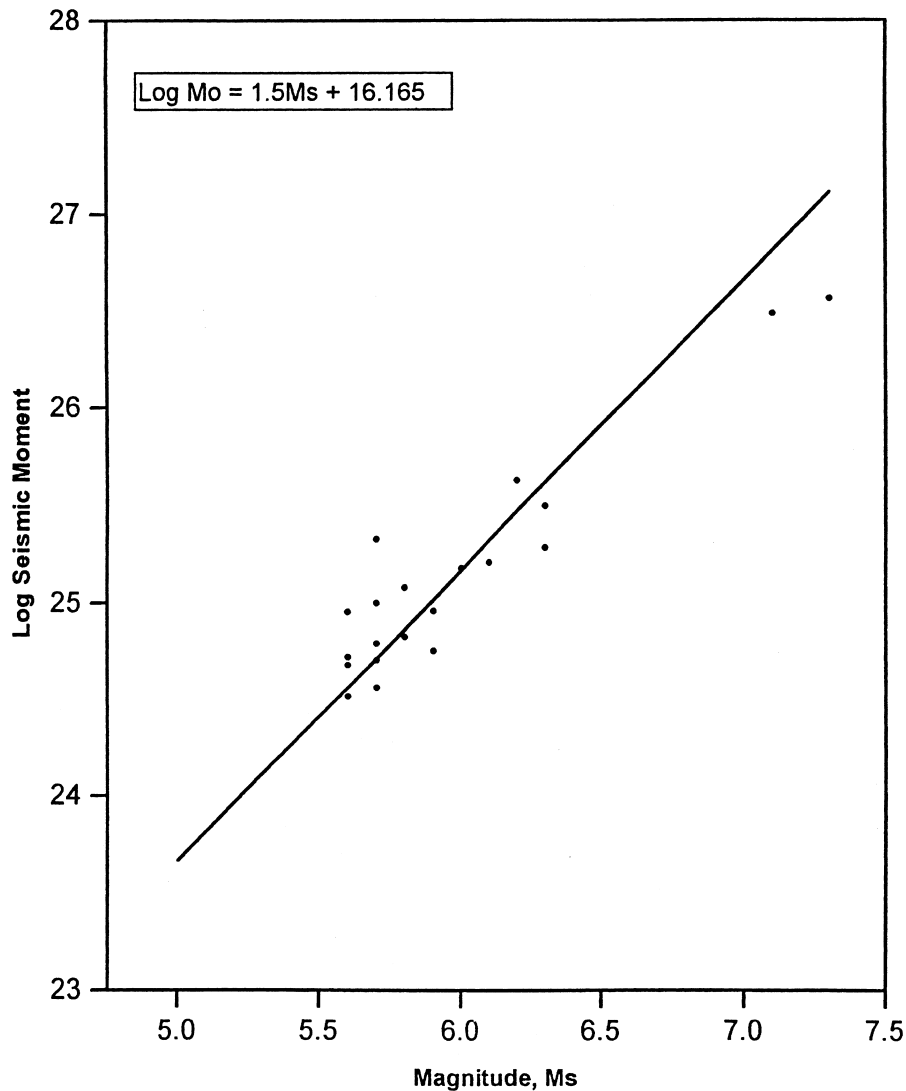


Fig. 4. Plot of the logarithm of seismic moment (M_0) versus surface wave magnitude for large shallow earthquakes in the Burmese arc region. See text for more details.

Table 3

Components of the strain rate $\dot{\epsilon}(\times 10^{-7}$ per year), velocity tensor \mathbf{U} (mm/yr) and eigen system of the velocity tensor for the 12 seismogenic sources in the region. Positive eigen values indicated tension while negative values indicate compression. Postive and negative plunge indicate that the eigen vector points into or out of the solid earth, respectively

Source	Elements of the strain rate tensor $\dot{\epsilon}$ (10^{-7} /yr)						Elements of the velocity tensor \mathbf{U} (mm/yr)						Eigen system of the velocity tensor (mm/yr)								
	11	12	13	22	23	33	11	12	13	22	23	33	λ_1	Az°	Pl°	λ_2	Az°	Pl°	λ_3	Az°	Pl°
1	-0.005	-0.001	-0.001	0.001	-0.002	0.004	-0.109	-0.044	-0.011	0.036	-0.017	0.020	-0.12 ± 0.01	16.2	-6.0	0.05 ± 0.00	103.8	-22.2	0.02 ± 0.00	120.5	66.9
2	-1.291	0.019	0.287	0.531	-0.438	0.761	-18.647	0.535	2.295	16.302	-3.503	3.042	-18.91 ± 2.49	358.5	6.2	17.17 ± 2.26	90.1	-13.9	2.44 ± 0.32	65.1	74.7
3	-0.17	-0.08	0.013	-0.02	0.166	0.196	-3.430	-2.982	0.092	-0.523	1.165	0.685	-5.38 ± 2.84	32.9	6.7	2.03 ± 1.07	118	36.2	0.08 ± 0.04	311.9	53.0
4	-0.006	-0.004	0.000	0.009	0.006	-0.003	-0.174	-0.067	0.000	0.150	0.029	-0.007	-0.19 ± 0.02	11.3	1.7	0.17 ± 0.01	101.1	9.3	-0.01 ± 0.00	291.6	-8.5
5	-0.108	-0.082	-0.001	0.158	0.109	-0.050	-2.556	-2.032	-0.007	2.312	0.544	-0.125	-3.30 ± 0.38	20.2	3.3	3.13 ± 0.36	109.7	9.0	-0.20 ± 0.02	309.9	-80.4
6	-0.005	-0.004	0.000	0.008	0.005	-0.002	-0.161	-0.123	0.000	0.136	0.026	-0.006	-0.21 ± 0.03	20.0	2.5	0.18 ± 0.03	109.6	7.4	-0.01 ± 0.00	308.2	-82.2
7	0.001	-0.001	0.001	0.000	0.002	-0.001	0.026	-0.031	0.007	0.007	0.012	-0.003	0.05 ± 0.0	323.0	-2.0	-0.03 ± 0.00	54.2	32.2	0.01 ± 0.00	49.9	57.7
8	0.001	-0.001	0.001	-0.003	0.001	0.002	0.027	-0.025	0.005	-0.038	0.007	0.004	0.04 ± 0.01	341.8	4.4	-0.05 ± 0.01	71.1	9.1	0.01 ± 0.00	97.1	79.9
9	0.006	-0.038	0.002	-0.029	0.005	0.023	0.260	-0.549	0.012	-0.296	0.025	0.058	0.60 ± 0.07	328.4	-0.3	-0.63 ± 0.08	58.5	2.3	0.06 ± 0.0	51.5	87.7
10	0.643	-0.463	0.152	-0.537	0.184	-0.107	26.454	-10.915	0.760	-9.207	0.920	-0.267	29.54 ± 4.76	344.3	0.9	-12.38 ± 1.99	74.2	5.2	-0.18 ± 0.02	84.5	-84.8
11	0.975	-0.702	0.230	-0.813	0.279	-0.162	52.227	-23.024	1.152	-9.611	1.395	-0.404	59.86 ± 8.07	341.7	0.6	-17.41 ± 2.34	71.6	-5.7	-0.24 ± 0.03	77.9	84.3
12	-0.085	-0.266	0.047	0.150	-0.043	-0.065	-6.108	-16.064	0.140	4.535	-0.129	-0.098	-17.71 ± 2.63	35.8	0.1	16.14 ± 2.40	125.8	-0.7	-0.10 ± 0.01	115.2	-89.3

The deformation pattern for each source given in the eigen system of velocity tensor in Table 3 is diagrammatically represented in Fig. 5. For a better understanding of the horizontal plate velocities, only those eigen vectors with plunge less than 25° are shown. The results for each seismogenic source are given in Fig. 5

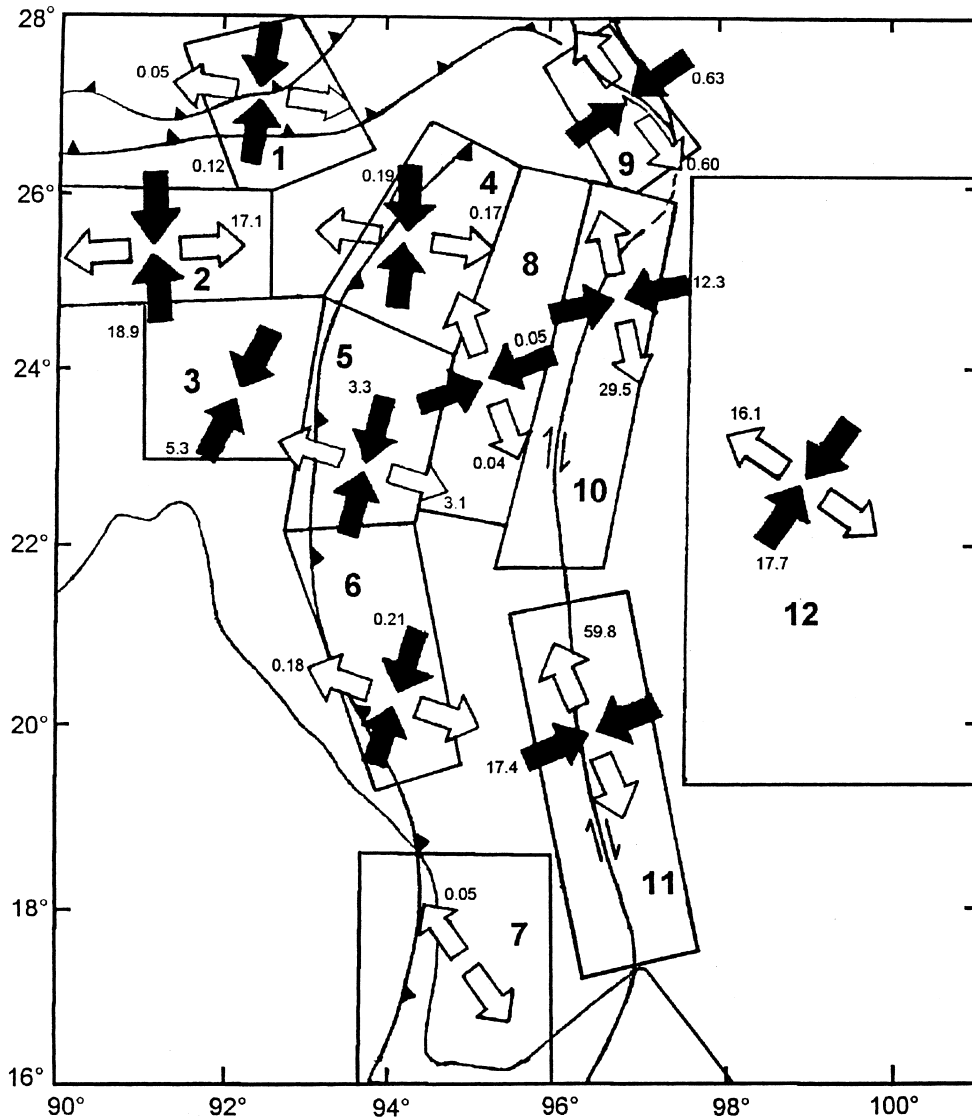


Fig. 5. Distribution of deformation velocities for the 12 seismogenic sources in the Burmese arc and adjacent regions. The values are in mm/yr. Converging arrows indicate compression while diverging arrows indicate extension.

4.1. Kopili–Bomdila fault zone in eastern Himalaya (source 1)

The Kopili and Bomdila faults have a general NW or WNW trend, running oblique to Main boundary thrust and Main central thrust in the eastern Himalayan region (Fig. 1). A total of 11 focal mechanisms are used in the moment tensor summation. Most of the solutions show left-lateral faulting indicating movements along the Kopili–Bomdila fault system. However, the complex interaction of these faults with the Himalayan trend results in events with dextral shear motion as well as thrust faulting as indicated by few mechanisms. The eigen system of the velocity tensor suggests a compressional deformation of 0.12 ± 0.01 mm/yr along $N16^\circ$ and an extension of 0.05 ± 0.004 mm/yr along $N104^\circ$ direction.

4.2. Shillong Plateau (source 2)

The region of Shillong Plateau, a prominent morphotectonic feature in northeast India, appears to be rising. The high seismic activity in this region is characterised by the occurrence of three $M > 7.0$ earthquakes including the great Shillong event of 1897. For the 1897 event, the re-estimated M_s value ($M_s = 8.0$) by Abe (1994) is considered in the present study. A total of 11 focal mechanism solutions have been used in the moment tensor summation. The eigen system of velocity tensor suggests compressional deformation of 18.9 ± 2.5 mm/yr in an almost NS direction and an EW extension of 17.1 ± 2.2 mm/yr. The vertical component suggests crustal thickening of 2.4 ± 0.3 mm/yr.

4.3. Tripura fold belt and Bengal basin (source 3)

The Tripura fold belt is an outer molasse basin containing thick folded Tertiary sediments (Mukhopadhyay and Dasgupta, 1988). While moderate seismicity is observed in the Tripura region, the seismicity is very low in Bengal basin except for the 1918 $M_s = 7.6$ Srimangal event (Kayal, 1997). Earthquakes in this region occur within the Indian plate just west of the Benioff zone. A total of six focal mechanisms showing thrust faulting have been used in the moment tensor summation. The results suggest compression of 5.4 ± 2.8 mm/yr along $N33^\circ$.

4.4. Indo-Burman ranges (Naga–Chin hills and Arakan–Yoma) (sources 4, 5 and 6)

The Indo-Burman ranges are one of the few intercontinental regions in the world where intermediate focus earthquakes occur. The seismic activity in this belt is intense and uniform to a depth of 200 km, but beyond $26^\circ N$ in the region of Naga hills the seismicity become shallow due to the collision process (Mitchell and McKerrow, 1975; Kayal, 1996). A large gravity anomaly along the Burmese arc is inferred as a subduction structure beneath the arc (Verma and Mukhopadhyay, 1977; Mukhopadhyay and Dasgupta, 1988; Gupta et al., 1990). The shallow earthquakes in this region show thrust as well as strike slip faulting. A total of 22 focal mechanism solutions occurring within the upper part of the plate have been used in the moment tensor summation. The eigen system of the velocity tensor suggests that in the Naga hills region (source 4), the deformation is taken up as a compression of 0.19 ± 0.02 mm/yr along $N11^\circ$ and an extension of 0.17 ± 0.01 mm/yr along $N101^\circ$, Chin hills region (source 5)

shows compression of 3.3 ± 0.4 mm/yr in the direction $N20^\circ$ and an extension of 3.1 ± 0.36 mm/yr in the direction $N110^\circ$, Arakan–Yoma region (source 6) shows a compression of 0.21 ± 0.03 mm/yr along $N20^\circ$ and an extension of 0.18 ± 0.03 mm/yr along $N110^\circ$.

4.5. Coastal Burma (source 7)

The region of Burmese coastal plains south of the latitude $18^\circ N$ is characterised by the absence of Benioff zone (Ni et al., 1989; Ravikumar and Rao, 1995) and the seismicity in this region is mainly confined to the overriding plate. A total of three focal mechanisms showing two normal faulting events and one with a minor strike-slip component have been used in the moment tensor summation. The eigen system of the velocity tensor suggest an extension of 0.05 mm/yr along $N323^\circ$.

4.6. Chindwin basin (source 8)

The earthquakes below Chindwin fore-arc basin occur within the overriding plate just above the subducting slab (Mukhopadhyay and Dasgupta, 1988). This region assumes significance in that these events define the complex deformation process in the vicinity of the subduction zone. All the four focal mechanism solutions show predominantly thrust faulting with one event showing a strike-slip component. The eigen system of the velocity tensor suggests an extension of 0.04 ± 0.01 mm/yr along $N342^\circ$ and compression of 0.05 ± 0.01 mm/yr along $N71^\circ$.

4.7. Mishmi thrust zone (source 9)

The Himalayan arc to the north and the Burmese arc to the east, meet at the Mishmi hills area and form a syntaxis zone. The great 1950 Assam earthquake ($M_s = 8.7$) occurred in the northern part of the syntaxis zone which shows right lateral strike-slip faulting (Ben-Menahem et al., 1974). Based on the focal mechanism solutions, Nandy and Dasgupta (1991) infer EW compressional stress in the Mishmi hills region. Mishmi thrust zone belongs to the southern part of the Himalayan syntaxis. A total of eight focal mechanism solutions showing predominantly strike-slip and thrust faulting events have been utilised in the moment tensor summation. The eigen system of the velocity tensor suggests a compressional deformation of 0.63 ± 0.08 mm/yr along $N58^\circ$ and an extension of 0.6 ± 0.07 mm/yr along $N328^\circ$.

4.8. Shan–Sagaing fault zone (sources 10 and 11)

The most prominent tectonic feature in the back-arc region is the Sagaing transform, a major right-lateral fault zone covering almost the whole length of the Burmese arc region (Fig. 1). Sources 10 and 11 cover this seismic belt and a total of 11 focal mechanism solutions showing right lateral strike-slip faulting have been used in the moment tensor summation. The eigen system of the velocity tensor suggests that in the northern part of the fault zone (source 10), a compressional deformation of 12.4 ± 1.9 mm/yr along $N74^\circ$ and an extension of 29.5 ± 4.7 mm/yr along $N344^\circ$ is taking place, while in the southern part of the fault zone a compressional deformation of 17.4 ± 2.3 mm/yr along $N71^\circ$ and an extension 59.8 ± 8.0 mm/yr

along $N341^\circ$ is observed. The U_{12} component of the velocity tensor calculated in the direction of the zone i.e., $N10^\circ$ for source 10 and $N170^\circ$ for source 11 indicate a shear velocity of 16.4 mm/yr in the northern part and 11 mm/yr in the southern part giving rise to an average shearing motion of 13.7 mm/yr along the fault.

4.9. Shan plateau (source 12)

East of the Sagaing fault within the Eastern Highlands (Shan plateau) in the SE Asian plate, seismicity is distributed over a wide zone in the continental interior along several active faults (Holt and Haines 1993). The region west of Red River fault in Shan plateau is characterised by left-lateral strike-slip faulting on NE oriented nodal planes with few normal faulting events occurring in the southern part of Lijiang fault. A total of 16 focal mechanism solutions have been utilised in the moment tensor summation. The eigen system of velocity tensor suggests a compression of 17.7 ± 2.6 mm/yr along $N36^\circ$ and an extension of 16.1 ± 2.4 mm/yr along $N126^\circ$.

5. Discussion

It can be seen from Fig. 5 that the NS oriented P axis in the eastern Himalayan region indicate continued northward compressive force within the Indian plate. However, the strike-slip component of motion along the Kopili–Bomdila faults which orient oblique to the trend of the Himalayas reveal that the present day crustal adjustment in this area is taking place through motion along these NW oriented fault systems. The results from the present study for Shillong Plateau suggests a NS trend compression and an EW directed tension. The NS compression can be due to back thrust from the Himalayas. The vertical component shows crustal thickening of about 2.4 ± 0.3 mm/yr. Rao and Kumar (1997) inferred that uplift of the Shillong Plateau is due to compressional forces from all sides of the plateau, one the NS directed force due to the Himalayan back thrust and the other, the EW directed resistance from the Burmese subduction.

The results for the Indo-Burman ranges in the overriding Burmese plate suggests dominantly strike-slip faulting with an average compressional direction of $N17^\circ$ (sources 4, 5 and 6) indicating either decoupling of the overriding plate from the Indian plate or oblique plate convergence. It is interesting to note that the Chin hills region, where the Burmese arc takes its maximum curvature shows a very high rate of deformation when compared to the Naga hills and Arakan–Yoma part of the arc. LeDain et al. (1984) suggest that convergence along the Indo-Burman ranges was active atleast until 1 Ma, while Satyabala (1998) inferred active subduction even at present below the Burmese arc. Ravikumar and Rao (1995) observed that P -axes for most of the mechanisms within the subducting slab are oriented in a NNE direction. Ni et al. (1989) suggest that the overriding plate is getting mechanically dragged northward along with the Indian plate and the present day convergence is accommodated by transcurrent movement along the Sagaing fault zone. Chen and Molnar (1990) believe that the Indo-Burman ranges decoupled from the Indian plate and northward displacement of these two together as a single unit is accommodated along the Sagaing fault. Since the above

observations are not conclusive enough with regard to active subduction below the Burmese arc, we believe that the Burma platelet is getting dragged along with the Indian plate and bring significant shearing motion along the Sagaing transform fault. The velocity tensor calculated in the direction of the fault shows an average dextral shear motion of 13.7 mm/yr along the Sagaing fault. This value is in good agreement with the slip rate of 15 mm/yr along the fault given by Molnar and Denq (1984). However, our estimate of 13.7 mm/yr obtained from the data of almost a 100 years is much smaller than the long term slip rate of 37 mm/yr for this fault proposed by Curray et al. (1979) based on sea floor spreading history in the Andaman Sea. Holt and Haines (1993) suggested that this discrepancy in slip rates for the Sagaing fault would vanish if there is no relative motion between south China and northern Eurasia. The velocities estimated in the present study are only from seismic events covering a period of 100 years and the total velocities should also include creep, an important deformation mechanism for near surface faults.

6. Conclusions

The shallow seismicity ($h \leq 70$ km) during 1897–1995, a good number of focal mechanism solutions and other morphotectonic details indicate that the Burmese arc and surrounding regions can be divided into 12 broad seismogenic zones of relatively homogeneous deformation. Active crustal deformation pattern obtained by summation of moment tensors for the identified seismogenic sources in general agree with the overall tectonics of the region. Certain salient results are given below:

The NS oriented *P*-axis in the eastern Himalayan region suggests continued northward compressive force within the Indian plate and strike-slip component of motion along the Kopili–Bomdila fault zone indicate crustal adjustments along the fault. The present study for Shillong Plateau suggests a NS compression trend of 18.9 mm/yr and an EW extension of 17.1 mm/yr. The vertical component in this region shows crustal thickening of about 2.4 mm/yr. The results for the Indo-Burman ranges indicate that the Burma platelet is getting dragged along with the Indian plate and the displacement of these together is accommodated along the Sagaing fault. The velocity tensor calculated in the direction of the Sagaing fault zone gives an average dextral shear motion of 13.7 mm/yr for the fault.

Acknowledgements

Financial assistance from UGC to one of the authors (T.D.S), in the form of a fellowship, is gratefully acknowledged. Critical comments and suggestions made by two anonymous reviewers have helped in improving the manuscript.

References

Abe, K., 1994. Instrumental magnitudes of historical earthquakes, 1892 to 1898. Bull. Seis. Soc. Am 84, 415–425.

- Aki, K., Richards, P., 1980. *Quantitative Seismology: Theory and Methods*. Freeman, San Francisco, CA, p. 557.
- Ben-Menahem, A., Abodi, E., Schild, R., 1974. The source of great Assam earthquake—an interplate wedge motion. *Phys. Earth Planet. Inter* 9, 265–289.
- Biswas, S., Dasgupta, A., 1986. Some observations on the mechanism of earthquakes in the Himalaya and the Burmese arc. *Tectonophys* 122, 325–343.
- Chandra, U., 1975. Seismicity, earthquake mechanisms and tectonics of Burma, 20°–28°N. *Geophys. J. Roy. Astr. Soc* 40, 367–381.
- Chandra, U., 1978. Seismicity, earthquake mechanisms along the Himalayan mountain range and vicinity. *Phys. Earth Planet. Inter* 16, 109–131.
- Chen, W.P., Molnar, P., 1990. Source parameters of earthquakes and intraplate deformation beneath the Shillong Plateau and northern Indo-Burman ranges. *J. Geophys. Res* 95, 12527–12552.
- Curry, J.R., Moore, D.G., Lawver, L., Emmel, E., Raith, R., Henry, M., Kieckhefer, R., 1979. Tectonics of the Andaman sea and Burma. *Am. Assoc. Pet. Geol. Mem* 29, 189–198.
- Fitch, T.J., 1970. Earthquake mechanisms in the Himalaya, Burmese and Andaman regions and continental tectonics in Central Asia. *J. Geophys. Res* 75, 2699–2709.
- Fitch, T.J., 1972. Plate convergence, transcurrent faults and internal deformation adjacent to southeast Asia and the western Pacific. *J. Geophys. Res* 77, 4432–4460.
- Geller, R.J., Kanamori, H., 1977. Magnitudes of great shallow earthquakes from 1902 to 1952. *Bull. Seis. Soc. Am* 67, 587–598.
- Gupta, H.K., Rajendran, K., Singh, H.N., 1986. Seismicity of northeast India region, Part I: The data base. *J. Geol. Soc. India* 28 (28), 335–365.
- Gupta, H.K., Fleitout, L., Froidevaux, C., 1990. Lithosphere subduction beneath the Arakan–Yoma fold belt: quantitative estimates using gravimetric and seismic data. *J. Geol. Soc. India* 35, 235–250.
- Gutenberg, G., Richter, C.F., 1954. *Seismicity of the Earth and its Associated Phenomena*. Princeton University Press, Princeton, NJ, p. 310.
- Haines, A.J., Holt, W.E., 1993. A procedure for obtaining the complete horizontal motions within zones of distributed deformation from the inversion of strain rate data. *J. Geophys. Res* 98, 12057–12082.
- Holt, W.E., Ni, J.F., Wallace, T.C., Haines, A.J., 1991. The active tectonics of the eastern Himalayan syntaxis and surrounding regions. *J. Geophys. Res* 96, 14595–14632.
- Holt, W.E., Haines, A.J., 1993. Velocity fields in deforming Asia from the inversion of earthquake released strains. *Tectonics* 12, 1–20.
- Jackson, J., McKenzie, D.P., 1988. The relationship between plate motion and seismic moment tensors, and the rates of active deformation in the Mediterranean and middle east. *Geophys. J* 93, 45–73.
- Kanamori, H., Anderson, D., 1975. Theoretical basis of empirical relations in seismology. *Bull. Seis. Soc. Am* 65, 1073–1095.
- Kayal, J.R., 1987. Microseismicity and source mechanism study: Shillong plateau, northeast India. *Bull. Seis. Soc. Am* 77, 184–194.
- Kayal, J.R., 1996. Earthquake source processes in northeast India—a review. *Himalayan Geol* 17, 53–69.
- Kayal, J.R. 1997. Seismicity of northeast India and surroundings development over the past 100 years. In: *The Great Shillong Earthquake 1897: A Centennial Retrospective*. Association of Exploration Geophys, Hyderabad, India.
- Kayal, J.R., De, R., Chakraborty, P., 1993. Microearthquakes at the main boundary thrust in Eastern Himalaya and the present tectonic model. *Tectonophys* 218, 375–381.
- Kiratzis, A., 1993. A study on the active crustal deformation of the north and east Anatolian fault zones. *Tectonophys* 218, 375–381.
- Kiratzis, A., Papazachos, C.B., 1995. Active crustal deformation from the Azores triple junction to the middle east. *Tectonophys* 243, 1–24.
- Kostrov, V.V., 1974. Seismic moment and energy of earthquakes and seismic flow of rocks. *Izv. Acad. Sci., USSR. Phys. Solid Earth* 1, 23–44.
- LeDain, A.Y., Tapponnier, P., Molnar, P., 1984. Active faulting and tectonics of Burma and surrounding regions. *J. Geophys. Res* 89, 452–472.
- Milne, W., Davenport, A., 1969. Determination of earthquake risk in Canada. *Bull. Seis. Soc. Am* 59, 729–754.

- Mitchell, A.H.G., McKerrow, W.S., 1975. Analogous evolution of the Burma orogen and the Scottish Caledonides. *Geol. Soc. Am. Bull.* 86, 305–315.
- Molnar, P., 1979. Earthquake recurrence intervals and plate tectonics. *Bull. Seis. Soc. Am.* 69, 115–133.
- Molnar, P., Denq, Q., 1984. Faulting associated with large earthquakes and the average rate of deformation in central and eastern Asia. *J. Geophys. Res.* 89, 6203–6228.
- Mukhopadhyay, M., Dasgupta, S., 1988. Deep structure and tectonics of the Burmese arc: constraints from earthquake and gravity data. *Tectonophysics* 149, 299–322.
- Mukhopadhyay, S., Chander, R., Khattri, K.N., 1993. Fine structure of seismotectonics in the western Shillong massif, northeastern India. *Proc. Ind. Acad. Sci.* 102, 383–398.
- Nandy, D.R., 1981. Tectonic pattern in northeast India—a discussion. *Ind. Jour. Earth Sci.* 8, 82–86.
- Nandy, D.R., 1986. Tectonics, seismicity and gravity of northeastern India and adjoining region. *Mem. Geo. Soc. Ind.* 119, 13–16.
- Nandy, D.R., Dasgupta, S., 1991. Seismotectonic domains of northeast India and adjacent areas. *Phys. Chem. Earth* 18, 371–384.
- Ni, J.F., Guzman-Speziale, M., Bevis, M., Holt, W.E., Wallace, T.C., Seager, W., 1989. Accretionary tectonics of Burma and three dimensional geometry of the Burma subduction zone. *Geology* 17, 68–71.
- Papazachos, B.C., 1990. Seismicity of the Aegean and surrounding area. *Tectonophysics* 178, 287–308.
- Papazachos, C.B., Kiratzi, A., 1992. A formulation for reliable estimation of active crustal deformation and its application to central Greece. *Geophys. J. Int.* 111, 424–432.
- Papazachos, C.B., Kiratzi, A., 1996. A detailed study of the active crustal deformation in the Aegean and surrounding area. *Tectonophysics* 253, 129–153.
- Papazachos, C.B., Kiratzi, A., Papazachos, B., 1992. Rates of active crustal deformation in the Aegean and the surrounding area. *J. Geodyn.* 16, 147–179.
- Rao, N.P., Kumar, M.R., 1997. Uplift and tectonics of the Shillong Plateau, northeast India. *J. Phys. Earth* 45, 167–176.
- Ravikumar, M., Rao, N.P., 1995. Significant trends related to the slab seismicity and tectonics in the Burmese arc region from Harvard CMT solutions. *Phys. Earth Planet. Inter.* 90, 75–80.
- Ravikumar, M., Rao, N.P., Chalam, S.V., 1996. A seismotectonic study of the Burma and Andaman arc regions using centroid moment tensor data. *Tectonophysics* 253, 155–168.
- Rothe, J.P., 1969. *The Seismicity of the Earth*. UNESCO, Paris pp. 336.
- Santo, T., 1969. On the characteristic seismicity in south Asia from Hindukush to Burma. *Bull. Inter. Inst. Seis. Earthquake Eng.* 6, 81–93.
- Satyabala, S.P., 1998. Subduction in the Indo-Burman region: is it still active? *Geophys. Res. Lett.* 25, 3189–3192.
- Satyabala, S.P., Gupta, H.K., 1996. Is the quiescence of major ($M = 7.5$) earthquakes since 1952 in the Himalaya and northeast India real? *Bull. Seis. Soc. Am.* 86, 1983–1986.
- Sipkin, S.A., Zirbes, M.D., 1996. Moment tensor solutions estimated using optimal filter theory: global seismicity 1994. *Phys. Earth Planet. Inter.* 93, 139–146.
- Verma, R.K., Krishnakumar, G.V.R., 1987. Seismicity and the nature of plate movement along the Himalayan arc, northeast India and Arakan–Yoma: a review. *Tectonophysics* 134, 153–175.
- Verma, R.K., Mukhopadhyay, M., 1977. An analysis of gravity field in northeast India. *Tectonophysics* 42, 282–317.
- Verma, R.K., Mukhopadhyay, M., Ahluwalia, M.S., 1976a. Earthquake mechanisms and tectonic features of northern Burma. *Tectonophysics* 32, 387–399.
- Verma, R.K., Mukhopadhyay, M., Ahluwalia, M.S., 1976b. Seismicity, gravity and tectonics of northeast India and northern Burma. *Bull. Seis. Soc. Am.* 66, 1683–1694.